

First observation of Cabibbo-suppressed Ξ_c^0 decays

R. Chistov,²⁰ I. Adachi,¹² H. Aihara,⁵⁸ D. M. Asner,⁴⁴ V. Aulchenko,³ T. Aushev,²⁰ A. M. Bakich,⁶⁷ A. Bala,⁴⁵
 V. Bhardwaj,³⁶ B. Bhuyan,¹⁴ A. Bondar,³ G. Bonvicini,⁶⁴ A. Bozek,⁴⁰ M. Bračko,^{29,21} J. Brodzicka,⁴⁰
 T. E. Browder,¹¹ V. Chekelian,³⁰ A. Chen,³⁷ P. Chen,³⁹ B. G. Cheon,¹⁰ K. Chilikin,²⁰ I.-S. Cho,⁶⁶ K. Cho,²⁴
 V. Chobanova,³⁰ Y. Choi,⁵¹ D. Cinabro,⁶⁴ M. Danilov,^{20,32} Z. Doležal,⁴ A. Drutskoy,^{20,32} D. Dutta,¹⁴ S. Eidelman,³
 D. Epifanov,⁵⁸ H. Farhat,⁶⁴ J. E. Fast,⁴⁴ M. Feindt,²³ T. Ferber,⁶⁸ A. Frey,⁹ V. Gaur,⁵³ N. Gabyshev,³
 S. Ganguly,⁶⁴ R. Gillard,⁶⁴ Y. M. Goh,¹⁰ B. Golob,^{28,21} J. Haba,¹² T. Hara,¹² K. Hayasaka,³⁵ H. Hayashii,³⁶
 Y. Horii,³⁵ Y. Hoshi,⁵⁶ W.-S. Hou,³⁹ H. J. Hyun,²⁶ T. Iijima,^{35,34} A. Ishikawa,⁵⁷ R. Itoh,¹² Y. Iwasaki,¹²
 T. Julius,³¹ D. H. Kah,²⁶ J. H. Kang,⁶⁶ E. Kato,⁵⁷ T. Kawasaki,⁴² H. Kichimi,¹² C. Kiesling,³⁰ D. Y. Kim,⁵⁰
 H. J. Kim,²⁶ J. B. Kim,²⁵ J. H. Kim,²⁴ K. T. Kim,²⁵ Y. J. Kim,²⁴ K. Kinoshita,⁵ J. Klucar,²¹ B. R. Ko,²⁵
 P. Kodyš,⁴ S. Korpar,^{29,21} P. Križan,^{28,21} T. Kumita,⁶⁰ A. Kuzmin,³ Y.-J. Kwon,⁶⁶ J. S. Lange,⁷ S.-H. Lee,²⁵
 J. Li,⁴⁹ Y. Li,⁶³ J. Libby,¹⁵ C. Liu,⁴⁸ Y. Liu,⁵ D. Liventsev,¹² P. Lukin,³ D. Matvienko,³ K. Miyabayashi,³⁶
 H. Miyata,⁴² R. Mizuk,^{20,32} G. B. Mohanty,⁵³ A. Moll,^{30,54} T. Mori,³⁴ N. Muramatsu,⁴⁷ R. Mussa,¹⁹ E. Nakano,⁴³
 M. Nakao,¹² Z. Natkaniec,⁴⁰ M. Nayak,¹⁵ E. Nedelkovska,³⁰ C. Ng,⁵⁸ S. Nishida,¹² O. Nitoh,⁶¹ S. Ogawa,⁵⁵
 S. Okuno,²² S. L. Olsen,⁴⁹ C. Oswald,² G. Pakhlova,²⁰ C. W. Park,⁵¹ H. Park,²⁶ H. K. Park,²⁶ R. Pestotnik,²¹
 M. Petrič,²¹ L. E. Piiilonen,⁶³ M. Ritter,³⁰ M. Röhrken,²³ A. Rostomyan,⁶⁸ H. Sahoo,¹¹ T. Saito,⁵⁷ K. Sakai,¹²
 Y. Sakai,¹² S. Sandilya,⁵³ D. Santel,⁵ L. Santelj,²¹ T. Sanuki,⁵⁷ V. Savinov,⁴⁶ O. Schneider,²⁷ G. Schnell,^{1,13}
 C. Schwanda,¹⁷ D. Semmler,⁷ K. Senyo,⁶⁵ O. Seon,³⁴ M. E. Sevier,³¹ M. Shapkin,¹⁸ C. P. Shen,³⁴ T.-A. Shibata,⁵⁹
 J.-G. Shiu,³⁹ B. Shwartz,³ A. Sibidanov,⁶⁷ F. Simon,^{30,54} Y.-S. Sohn,⁶⁶ A. Sokolov,¹⁸ E. Solovieva,²⁰ M. Starič,²¹
 M. Steder,⁶⁸ M. Sumihama,⁸ T. Sumiyoshi,⁶⁰ U. Tamponi,^{19,62} K. Tanida,⁴⁹ G. Tatishvili,⁴⁴ Y. Teramoto,⁴³
 M. Uchida,⁵⁹ T. Uglov,^{20,33} Y. Unno,¹⁰ S. Uno,¹² P. Urquijo,² Y. Usov,³ S. E. Vahsen,¹¹ C. Van Hulse,¹
 P. Vanhoefer,³⁰ G. Varner,¹¹ K. E. Varvell,⁶⁷ A. Vinokurova,³ M. N. Wagner,⁷ C. H. Wang,³⁸ M.-Z. Wang,³⁹
 P. Wang,¹⁶ X. L. Wang,⁶³ Y. Watanabe,²² K. M. Williams,⁶³ E. Won,²⁵ B. D. Yabsley,⁶⁷ J. Yamaoka,¹¹
 Y. Yamashita,⁴¹ S. Yashchenko,⁶⁸ Y. Yook,⁶⁶ Y. Yusa,⁴² Z. P. Zhang,⁴⁸ V. Zhilich,³ V. Zhulanov,³ and A. Zupanc²³

(The Belle Collaboration)

¹University of the Basque Country UPV/EHU, 48080 Bilbao

²University of Bonn, 53115 Bonn

³Budker Institute of Nuclear Physics SB RAS and Novosibirsk State University, Novosibirsk 630090

⁴Faculty of Mathematics and Physics, Charles University, 121 16 Prague

⁵University of Cincinnati, Cincinnati, Ohio 45221

⁶Deutsches Elektronen-Synchrotron, 22607 Hamburg

⁷Justus-Liebig-Universität Gießen, 35392 Gießen

⁸Gifu University, Gifu 501-1193

⁹II. Physikalisches Institut, Georg-August-Universität Göttingen, 37073 Göttingen

¹⁰Hanyang University, Seoul 133-791

¹¹University of Hawaii, Honolulu, Hawaii 96822

¹²High Energy Accelerator Research Organization (KEK), Tsukuba 305-0801

¹³Ikerbasque, 48011 Bilbao

¹⁴Indian Institute of Technology Guwahati, Assam 781039

¹⁵Indian Institute of Technology Madras, Chennai 600036

¹⁶Institute of High Energy Physics, Chinese Academy of Sciences, Beijing 100049

¹⁷Institute of High Energy Physics, Vienna 1050

¹⁸Institute for High Energy Physics, Protvino 142281

¹⁹INFN - Sezione di Torino, 10125 Torino

²⁰Institute for Theoretical and Experimental Physics, Moscow 117218

²¹J. Stefan Institute, 1000 Ljubljana

²²Kanagawa University, Yokohama 221-8686

²³Institut für Experimentelle Kernphysik, Karlsruher Institut für Technologie, 76131 Karlsruhe

²⁴Korea Institute of Science and Technology Information, Daejeon 305-806

²⁵Korea University, Seoul 136-713

²⁶Kyungpook National University, Daegu 702-701

²⁷École Polytechnique Fédérale de Lausanne (EPFL), Lausanne 1015

²⁸Faculty of Mathematics and Physics, University of Ljubljana, 1000 Ljubljana

²⁹University of Maribor, 2000 Maribor

³⁰Max-Planck-Institut für Physik, 80805 München

³¹School of Physics, University of Melbourne, Victoria 3010

- ³²*Moscow Physical Engineering Institute, Moscow 115409*
- ³³*Moscow Institute of Physics and Technology, Moscow Region 141700*
- ³⁴*Graduate School of Science, Nagoya University, Nagoya 464-8602*
- ³⁵*Kobayashi-Maskawa Institute, Nagoya University, Nagoya 464-8602*
- ³⁶*Nara Women's University, Nara 630-8506*
- ³⁷*National Central University, Chung-li 32054*
- ³⁸*National United University, Miao Li 36003*
- ³⁹*Department of Physics, National Taiwan University, Taipei 10617*
- ⁴⁰*H. Niewodniczanski Institute of Nuclear Physics, Krakow 31-342*
- ⁴¹*Nippon Dental University, Niigata 951-8580*
- ⁴²*Niigata University, Niigata 950-2181*
- ⁴³*Osaka City University, Osaka 558-8585*
- ⁴⁴*Pacific Northwest National Laboratory, Richland, Washington 99352*
- ⁴⁵*Panjab University, Chandigarh 160014*
- ⁴⁶*University of Pittsburgh, Pittsburgh, Pennsylvania 15260*
- ⁴⁷*Research Center for Electron Photon Science, Tohoku University, Sendai 980-8578*
- ⁴⁸*University of Science and Technology of China, Hefei 230026*
- ⁴⁹*Seoul National University, Seoul 151-742*
- ⁵⁰*Soongsil University, Seoul 156-743*
- ⁵¹*Sungkyunkwan University, Suwon 440-746*
- ⁵²*School of Physics, University of Sydney, New South Wales 2006*
- ⁵³*Tata Institute of Fundamental Research, Mumbai 400005*
- ⁵⁴*Excellence Cluster Universe, Technische Universität München, 85748 Garching*
- ⁵⁵*Toho University, Funabashi 274-8510*
- ⁵⁶*Tohoku Gakuin University, Tagajo 985-8537*
- ⁵⁷*Tohoku University, Sendai 980-8578*
- ⁵⁸*Department of Physics, University of Tokyo, Tokyo 113-0033*
- ⁵⁹*Tokyo Institute of Technology, Tokyo 152-8550*
- ⁶⁰*Tokyo Metropolitan University, Tokyo 192-0397*
- ⁶¹*Tokyo University of Agriculture and Technology, Tokyo 184-8588*
- ⁶²*University of Torino, 10124 Torino*
- ⁶³*CNP, Virginia Polytechnic Institute and State University, Blacksburg, Virginia 24061*
- ⁶⁴*Wayne State University, Detroit, Michigan 48202*
- ⁶⁵*Yamagata University, Yamagata 990-8560*
- ⁶⁶*Yonsei University, Seoul 120-749*
- ⁶⁷*School of Physics, University of Sydney, NSW 2006*
- ⁶⁸*Deutsches Elektronen-Synchrotron, 22607 Hamburg*

We report the first observation of the Cabibbo-suppressed decays $\Xi_c^0 \rightarrow \Xi^- K^+$, $\Xi_c^0 \rightarrow \Lambda K^+ K^-$ and $\Xi_c^0 \rightarrow \Lambda \phi$, using a data sample of 711 fb^{-1} collected at the $\Upsilon(4S)$ resonance with the Belle detector at the KEKB asymmetric-energy e^+e^- collider. We measure the ratios of branching fractions to be $\frac{\mathcal{B}(\Xi_c^0 \rightarrow \Xi^- K^+)}{\mathcal{B}(\Xi_c^0 \rightarrow \Xi^- \pi^+)} = (2.75 \pm 0.51 \pm 0.25) \times 10^{-2}$, $\frac{\mathcal{B}(\Xi_c^0 \rightarrow \Lambda K^+ K^-)}{\mathcal{B}(\Xi_c^0 \rightarrow \Xi^- \pi^+)} = (2.86 \pm 0.61 \pm 0.37) \times 10^{-2}$ and $\frac{\mathcal{B}(\Xi_c^0 \rightarrow \Lambda \phi)}{\mathcal{B}(\Xi_c^0 \rightarrow \Xi^- \pi^+)} = (3.43 \pm 0.58 \pm 0.32) \times 10^{-2}$, where the first uncertainty is statistical and the second is systematic.

PACS numbers: 14.20.Lq, 13.30.Eg

Weak decays of charmed baryons provide a useful test of many competing theoretical models and approaches [1]. While many Cabibbo-favored decays of Λ_c^+ and $\Xi_c^{+,0}$ have been observed, the accuracy of the measured branching fractions remains poor. Some of the Cabibbo-suppressed (CS) decays of the Λ_c^+ were observed by Belle [2] and *BABAR* [3]; no experimental information is available for the CS decay modes of the Ξ_c^0 . In this paper we report the first observation of the CS decays $\Xi_c^0 \rightarrow \Xi^- K^+$, $\Xi_c^0 \rightarrow \Lambda K^+ K^-$ and $\Xi_c^0 \rightarrow \Lambda \phi$. The first decay is the Cabibbo-suppressed analogue of the Cabibbo-favored decay $\Xi_c^0 \rightarrow \Xi^- \pi^+$ and proceeds through the external W -emission and W -exchange diagrams (see the two up-

per panels of Fig. 1). The third one proceeds through the internal W -emission and W -exchange diagrams (see lower two panels of Fig. 1). The $\Xi_c^0 \rightarrow \Lambda K^+ K^-$ decay can receive contributions from all W -mediated diagrams. The W -internal diagrams in charmed meson decays are usually color suppressed; this is not the case in charmed baryon decays [4]. Therefore, it is important to check this behavior in Cabibbo-suppressed Ξ_c^0 decays.

The analysis is performed using data collected with the Belle detector at the KEKB asymmetric-energy e^+e^- collider [5]. The data sample consists of 711 fb^{-1} taken at the $\Upsilon(4S)$ resonance.

The Belle detector is a large-solid-angle magnetic spec-

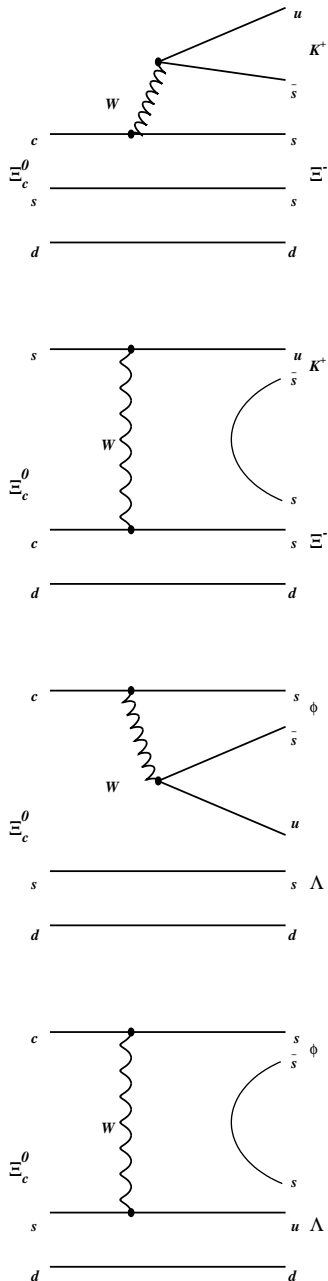


FIG. 1: Diagrams for the $\Xi_c^0 \rightarrow \Xi^- K^+$ (upper two) and $\Xi_c^0 \rightarrow \Lambda \phi$ (lower two) decays.

trometer that consists of a silicon vertex detector, a 50-layer central drift chamber (CDC), an array of aerogel threshold Cherenkov counters (ACC), a barrel-like arrangement of time-of-flight scintillation counters (TOF), and an electromagnetic calorimeter composed of CsI(Tl) crystals located inside a superconducting solenoid coil that provides a 1.5 T magnetic field. An iron flux return located outside of the coil is instrumented to detect K_L^0

mesons and to identify muons. The detector is described in detail elsewhere [6].

We select charged pions, kaons and protons (unless a track has been identified as a daughter of a Ξ^- or Λ hyperon) that originate from the region $dr < 0.5$ cm and $|dz| < 1$ cm, where dr and dz are the distances between the point of closest approach and the interaction point (IP) in the plane perpendicular to the beam axis (the r - ϕ plane) and along the beam direction (z), respectively. We apply identification (ID) requirements for the charged particles using likelihoods \mathcal{L}_K , \mathcal{L}_π and \mathcal{L}_p for the kaon, pion and proton hypotheses, respectively, that are derived from information recorded by the TOF, ACC and CDC. Charged kaons are required to satisfy $\mathcal{L}_K/(\mathcal{L}_K + \mathcal{L}_\pi) > 0.6$ and $\mathcal{L}_K/(\mathcal{L}_K + \mathcal{L}_p) > 0.6$. Protons are required to satisfy $\mathcal{L}_p/(\mathcal{L}_K + \mathcal{L}_p) > 0.6$ and $\mathcal{L}_p/(\mathcal{L}_\pi + \mathcal{L}_p) > 0.6$. For both species, these criteria have an efficiency greater than 87% and a misidentification probability of less than 11%. We apply no ID requirements for pions.

In our Monte Carlo (MC) simulation, Ξ_c^0 baryons are produced in $e^+e^- \rightarrow c\bar{c}$ events using the PYTHIA [7] fragmentation package. Subsequent short-lived particle decays at the IP are generated by EvtGen [7]. The detailed detector response is simulated using GEANT [8].

The Λ hyperons are reconstructed in the decay mode $\Lambda \rightarrow p\pi^-$. (Unless stated otherwise, charge conjugation is implicitly assumed throughout the paper.) We fit the p and π^- tracks to a common vertex and require an invariant mass in a $\pm 3 \text{ MeV}/c^2$ ($\approx \pm 3\sigma$) interval around the nominal Λ mass. We then impose the following requirements on the Λ decay vertex: the vertex fit must be satisfactory; the difference in the z coordinates of the proton and pion at the decay vertex must satisfy $\Delta z < 1$ cm; the distance between the Λ decay vertex position and IP in the r - ϕ plane must be greater than 0.1 cm; the angle α_Λ between the Λ momentum vector and the vector joining the IP to the decay vertex must satisfy $\cos \alpha_\Lambda > 0.9$ for the case $\Xi_c^0 \rightarrow \Lambda \phi$. (No $\cos \alpha_\Lambda$ requirement is applied for the $\Xi_c^0 \rightarrow \Xi^- K^+$ candidates since, in this case, we select Λ 's emerging from the Ξ^- decay vertex rather than the IP.)

The Ξ^- hyperons are reconstructed in the decay mode $\Xi^- \rightarrow \Lambda \pi^-$. We require a $\Lambda \pi^-$ invariant mass within a $\pm 6 \text{ MeV}/c^2$ ($\approx \pm 3\sigma$) interval around the nominal Ξ^- mass, fit the Λ and the π^- track to a common vertex and apply the following requirements: the vertex fit must be satisfactory; the distance between the Ξ^- decay vertex position and IP in the r - ϕ plane must be greater than 0.1 cm; the angle α_{Ξ^-} between the Ξ^- momentum vector and the vector joining the IP to the Ξ^- decay vertex must satisfy $\cos \alpha_{\Xi^-} > 0.9$. All criteria described above and the reconstruction method for the two long-lived hyperons have been verified and used in previous Belle papers on Λ , Ξ^- and Ω^- hyperons [2, 9–11].

The combinatorial background peaks at low momenta

while charmed hadrons in $e^+e^- \rightarrow c\bar{c}$ are concentrated at high momenta. Therefore, the momentum p^* in the e^+e^- center-of-mass frame for the Ξ_c^0 candidates is required to be greater than $3.0 \text{ GeV}/c$.

We reconstruct $\Xi_c^0 \rightarrow \Xi^- K^+$ candidates by combining Ξ^- and K^+ candidates in the event. The resulting spectrum of the invariant mass $M(\Xi^- K^+)$ after all selection requirements is shown in Fig. 2, where a signal near $2470 \text{ MeV}/c^2$ is observed. In addition, a broad bump above the combinatorial background is evident at higher mass that is due to a reflection from $\Xi_c^0 \rightarrow \Xi^- \pi^+$, in which the pion is misidentified as a kaon. We first check the origin of this reflection peak with data. With tight kaon ID requirements, the reflection bump completely vanishes; with looser ID requirements, the peak is more prominent. We check the shape and position of the reflection using signal MC events for the decay $\Xi_c^0 \rightarrow \Xi^- \pi^+$. By reconstructing such events as $\Xi^- K^+$, we observe that the position and shape of this reflection match those of the data. We also check the invariant mass distribution for the wrong-sign $\Xi^- K^-$ combinations in data with the same selection requirements. We find no indications of peaking structures and observe a mass distribution that is featureless over a wide mass range centered around the mass of the Ξ_c^0 (see Fig. 3).

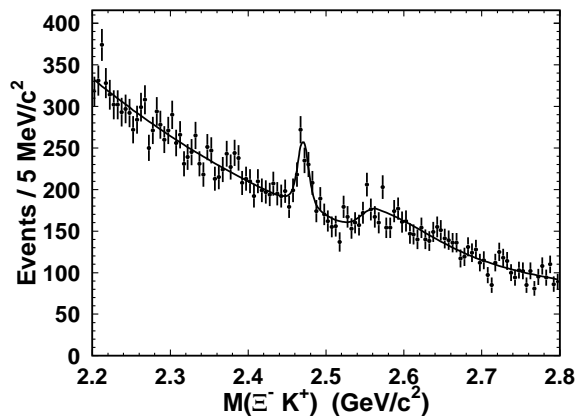


FIG. 2: Fitted $M(\Xi^- K^+)$ spectrum. The peak at $2470 \text{ MeV}/c^2$ corresponds to the $\Xi_c^0 \rightarrow \Xi^- K^+$ signal. The broad structure from $2520 \text{ MeV}/c^2$ to $2700 \text{ MeV}/c^2$ corresponds to the $\Xi_c^0 \rightarrow \Xi^- \pi^+$. The smooth curve is the fit result, described in the text.

The solid curve in Fig. 2 is the result of the fit that includes the signal, the reflection and the combinatorial background. Here and elsewhere in this paper, we use a binned maximum likelihood fit. The signal is described by a double Gaussian with a common floating mean and widths fixed from signal MC events. We calibrate these widths by the data-to-MC ratios from the study of $\Xi_c^0 \rightarrow \Xi^- \pi^+$ decay: we take σ_{core} and σ_{tail} from the fit to the $\Xi_c^0 \rightarrow \Xi^- \pi^+$ signal on data and di-

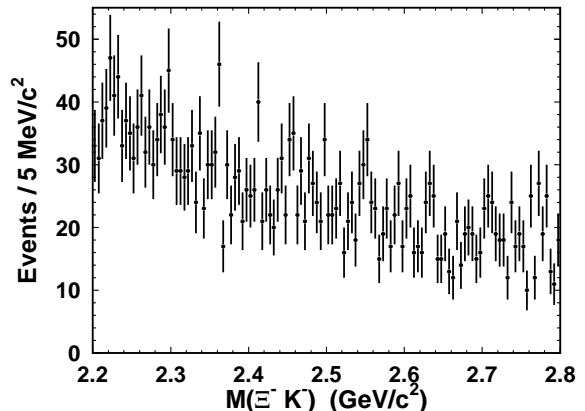


FIG. 3: The wrong-sign $M(\Xi^- K^-)$ spectrum. There are no peaking structures around $2470 \text{ MeV}/c^2$.

vide these by the corresponding σ 's from its signal MC events: $(\frac{\sigma_{\text{data}}}{\sigma_{\text{mc}}})_{\Xi^- \pi^+} = 6.00/5.48 = 1.09$, $(\frac{\sigma_{\text{data}}}{\sigma_{\text{mc}}})_{\Xi^- \pi^+} = 12.50/11.06 = 1.13$. Then we make a correction of σ_{core} and σ_{tail} taken from $\Xi_c^0 \rightarrow \Xi^- K^+$ MC events and obtain the widths that we fix in the fit of the $\Xi_c^0 \rightarrow \Xi^- K^+$ signal on data: $(\sigma_{\text{core}}^{\text{data}})_{\Xi^- K^+} = 1.09 \times 5.87 = 6.43 \text{ MeV}/c^2$, $(\sigma_{\text{tail}}^{\text{data}})_{\Xi^- K^+} = 1.13 \times 12.72 = 14.35 \text{ MeV}/c^2$. We also include the shape of the reflection from $\Xi_c^0 \rightarrow \Xi^- \pi^+$ that is determined from MC-generated $\Xi_c^0 \rightarrow \Xi^- \pi^+$ decays reconstructed as $\Xi_c^0 \rightarrow \Xi^- K^+$. We find that the reflection can be parametrized by an asymmetric Gaussian with the right shoulder being larger than the left one. We fix the shape of the reflection and leave its normalization as a free parameter in the fit. The background is parametrized by a third-order polynomial function. The fit yields $N = 313.8 \pm 57.8$ events and $M = 2470.6 \pm 1.5 \text{ MeV}/c^2$ for the $\Xi_c^0 \rightarrow \Xi^- K^+$ signal. The obtained mass is in good agreement with the world average mass of $M(\Xi_c^0) = (2470.88^{+0.34}_{-0.80}) \text{ MeV}/c^2$ [4]. The significance of the observed signal is 8.0σ . The signal significance reported here and elsewhere in this paper is determined from $2 \cdot \ln(\mathcal{L}_0/\mathcal{L}_{\text{max}})$, where \mathcal{L}_{max} is the maximum likelihood for the nominal fit and \mathcal{L}_0 is the corresponding value with the signal yield fixed to zero. The extraction of the significance takes into account 2 additional degrees of freedom (mass and yield).

We generate signal MC events without any momentum requirement, so here and elsewhere in this paper all calculated efficiencies take into account the kinematic efficiency of the $p^* > 3.0 \text{ GeV}/c$ requirement. The measured total reconstruction efficiency for the $\Xi_c^0 \rightarrow \Xi^- K^+$ mode is $(4.47 \pm 0.03)\%$; this includes the intermediate branching fraction $\mathcal{B}(\Lambda \rightarrow p\pi^-)$ [4]. Using the results from the study of the normalization channel $\Xi_c^0 \rightarrow \Xi^- \pi^+$ (the number of events and reconstruction efficiency, described below), we obtain the ratio $\frac{\mathcal{B}(\Xi_c^0 \rightarrow \Xi^- K^+)}{\mathcal{B}(\Xi_c^0 \rightarrow \Xi^- \pi^+)} = (2.75 \pm 0.51 \pm$

$0.25) \times 10^{-2}$. The first and second errors are statistical and systematic, respectively.

In the search for $\Xi_c^0 \rightarrow \Lambda\phi(\phi \rightarrow K^+K^-)$ decay, in addition to the above-described selection criteria, we require that the mass of the ΛK^- pair be outside a ± 6.5 MeV/ c^2 mass window around $M(\Omega^-) = 1672.45$ MeV/ c^2 [4]. This requirement removes the contribution from the well-known $\Xi_c^0 \rightarrow \Omega^- K^+$ ($\Omega^- \rightarrow \Lambda K^-$) decay [4]. The resulting spectrum of the three-body invariant mass $M(\Lambda K^+ K^-)$ is shown in Fig. 4, where a signal near 2470 MeV/ c^2 is observed. We fit the $\Xi_c^0 \rightarrow \Lambda K^+ K^-$ signal to the data with a double Gaussian with the fixed widths from corresponding MC events ($\sigma_{\text{core}} = 2.53$ MeV/ c^2 , $\sigma_{\text{tail}} = 6.10$ MeV/ c^2). For the background, we use a third-order polynomial. The fit results in a mass of $M = 2471.2 \pm 1.1$ MeV/ c^2 and a yield of $N = 511.0 \pm 109.5$. This mass is in good agreement with the world average mass of the Ξ_c^0 . The significance of this signal is 6.4σ .

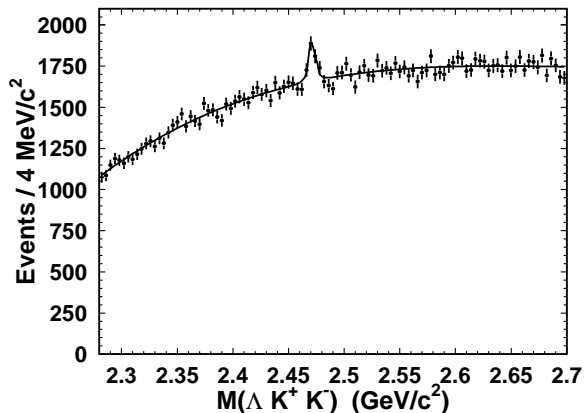


FIG. 4: The $M(\Lambda K^+ K^-)$ distribution together with the overlaid fitting curve. The fit is described in the text.

To obtain the $\Xi_c^0 \rightarrow \Lambda\phi$ signal, we select $\Lambda K^+ K^-$ combinations within the ± 12 MeV/ c^2 mass window around $M(\Xi_c^0) = 2470.9$ MeV/ c^2 and investigate the distribution of $M(K^+ K^-)$ shown by the data points in Fig. 5. The superimposed histogram shows the ϕ signal for the events taken from the Ξ_c^0 sidebands, which are normalized to the area under the Ξ_c^0 signal. The left Ξ_c^0 sideband is defined by 2403.2 MeV/ $c^2 < M(\Lambda K^+ K^-) < 2451.2$ MeV/ c^2 , and the right one by 2491.2 MeV/ $c^2 < M(\Lambda K^+ K^-) < 2539.2$ MeV/ c^2 . A distinct excess of ϕ mesons is observed in the Ξ_c^0 signal region, establishing the observation of the two-body $\Xi_c^0 \rightarrow \Lambda\phi$ decay.

The ϕ signal is described by a Breit-Wigner function convolved with the double Gaussian resolution function with the widths fixed from MC events ($\sigma_{\text{core}} = 0.61$ MeV/ c^2 , $\sigma_{\text{tail}} = 1.39$ MeV/ c^2). The natural width Γ_ϕ is fixed to its nominal value of 4.26 MeV [4]. The

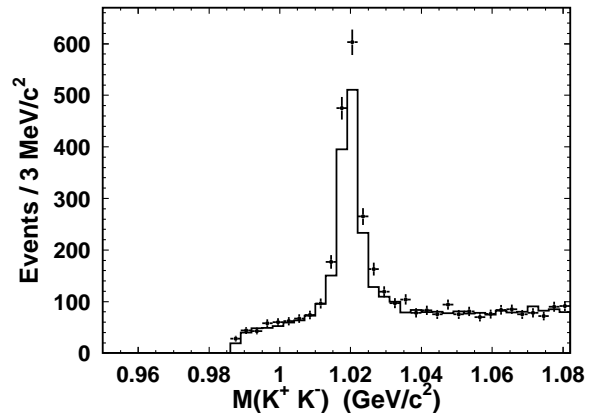


FIG. 5: The $M(K^+ K^-)$ distributions. Cross points with error bars represent the events within the ± 12 MeV/ c^2 mass window around $M(\Lambda K^+ K^-) = 2471.2$ MeV/ c^2 . The solid histogram shows the ϕ signal for the events taken from the normalized Ξ_c^0 sidebands (see the text).

threshold function multiplied by a third-order polynomial is used to model the combinatorial background together with a nonresonant contribution. The fit results in the following ϕ yields: $N_1 = 1533.1 \pm 47.9$ events in the Ξ_c^0 signal region and $N_2 = 5006.8 \pm 88.8$ events in the Ξ_c^0 sidebands region. From this, the final net ϕ yield in $\Xi_c^0 \rightarrow \Lambda K^+ K^-$ decays is $N_\phi = (N_1 \pm \delta N_1)/0.98 - (N_2 \pm \delta N_2) \times 0.249 = 315.8 \pm 53.7$. The coefficient 0.98 takes into account the efficiency of the mass requirement of ± 12 MeV/ c^2 around $M(\Xi_c^0)$. The coefficient 0.249 is the ratio of areas under the Ξ_c^0 signal and the sum of its sidebands. From the obtained ϕ net yield and the probability value of the Gaussian distribution of the error, we extract a significance of 5.9σ for the $\Xi_c^0 \rightarrow \Lambda\phi$ signal. By varying the width of the Ξ_c^0 sidebands and repeating the ϕ yield extraction procedure, we obtain significances that are never less than 5.6σ . We quote this latter value as our significance of the $\Xi_c^0 \rightarrow \Lambda\phi$ signal, including the systematic error. The total reconstruction efficiency, including the intermediate branching fractions of $\Lambda \rightarrow p\pi^-$ and $\phi \rightarrow K^+ K^-$ is extracted from signal MC events to be $(3.60 \pm 0.02)\%$. We obtain $\frac{\mathcal{B}(\Xi_c^0 \rightarrow \Lambda\phi)}{\mathcal{B}(\Xi_c^0 \rightarrow \Xi^- \pi^+)} = (3.43 \pm 0.58 \pm 0.32) \times 10^{-2}$. The first and second errors are statistical and systematic, respectively.

To obtain the ratio of branching fractions for the three-body $\Xi_c^0 \rightarrow \Lambda K^+ K^-$ channel, we estimate its signal efficiency as follows. Taking into account the correspondence between the obtained number of events for the three-body mode (511.0 ± 109.5) and for the $\Xi_c^0 \rightarrow \Lambda\phi$ mode (315.8 ± 53.7), we generate a sample of Ξ_c^0 states that decay 40% of the time into the three-body phase space $\Lambda K^+ K^-$ final state and 60% of the time into the $\Lambda\phi$ final state. The total reconstruction efficiency, includ-

ing the intermediate branching fraction for $\Lambda \rightarrow p\pi^-$, is found to be $(7.01 \pm 0.04)\%$. We vary the portion of the resonant mode over a $\pm 50\%$ range and repeat the efficiency extraction. The absolute value of the largest variation in the total reconstruction efficiency is found to be 0.15%, which is treated as a systematic error. Finally, we get $\frac{\mathcal{B}(\Xi_c^0 \rightarrow \Lambda K^+ K^-)}{\mathcal{B}(\Xi_c^0 \rightarrow \Xi^- \pi^+)} = (2.86 \pm 0.61 \pm 0.37) \times 10^{-2}$, where the first and second errors are statistical and systematic, respectively. An additional source of systematic error due to the MC model of Ξ_c^0 decay into the final state $\Lambda K^+ K^-$ is also included.

Currently, there are no absolute branching fraction measurements for Ξ_c^0 , so we choose to normalize the results for Ξ_c^0 decays to the well-known decay mode $\Xi_c^0 \rightarrow \Xi^- \pi^+$. Using the same data sample, the selection criteria and the $p(\Xi_c^0)^* > 3.0$ GeV/ c requirement described above, we reconstruct $\Xi_c^0 \rightarrow \Xi^- \pi^+$ decays and obtain the $M(\Xi^- \pi^+)$ spectrum shown in Fig. 6. We fit this spectrum with a double Gaussian with a floating common mean and floating widths (to describe the signal) and a third-order polynomial function to account for the background. The signal yield is $N = 15324 \pm 262$. The Gaussian widths and common mean are extracted from the fit to be $\sigma_{\text{core}} = 6.0 \pm 0.3$ MeV/ c^2 , $\sigma_{\text{tail}} = 12.5 \pm 0.8$ MeV/ c^2 and $M = 2471.4 \pm 0.1$ MeV/ c^2 , respectively. The mass is in agreement with the world average value: $M(\Xi_c^0) = (2470.88_{-0.80}^{+0.34})$ MeV/ c^2 [4]. We generate signal MC events and reconstruct the generated events according to the procedure that is used in analyzing the data. The total reconstruction efficiency is determined to be $(6.00 \pm 0.03)\%$. This efficiency includes the intermediate branching fraction $\mathcal{B}(\Lambda \rightarrow p\pi^-)$ [4]. Since the number of signal events for this mode is large, we do not fix the Gaussian resolution to obtain the final yield for $\Xi_c^0 \rightarrow \Xi^- \pi^+$.

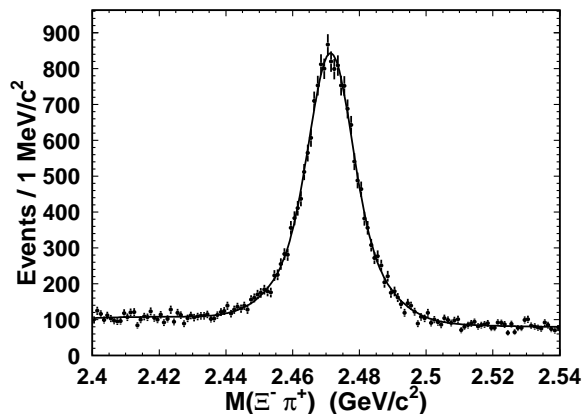


FIG. 6: The $M(\Xi^- \pi^+)$ distribution for data together with the overlaid fitting curve. The fit is described in the text.

We consider the following sources of systematic errors:

the fit, K ID efficiency and MC statistics. The fit systematics are determined by varying the range of the fitted invariant mass distributions and by changing the polynomial order for the background function. Other sources of uncertainties, such as particle reconstruction efficiency and Λ reconstruction efficiency, cancel in the branching fraction ratio. For the $\Xi_c^0 \rightarrow \Lambda\phi$ and $\Xi_c^0 \rightarrow \Lambda K^+ K^-$ results, we consider possible interference between the non- ϕ $\Lambda K^+ K^-$ and resonant $\Lambda\phi(\phi \rightarrow K^+ K^-)$ amplitudes. This effect is estimated to be 3.8%. Finally, the MC model of the $\Xi_c^0 \rightarrow \Lambda K^+ K^-$ mode introduces an additional uncertainty that we estimate to be 2%. As we do not have a calibration channel for the width correction in the $\Xi_c^0 \rightarrow \Lambda K^+ K^-$ mode, we add a 10% systematic error based on the calculated corrections in the $\Xi_c^0 \rightarrow \Xi^- \pi^+$ mode. Table I summarizes the systematic errors.

In conclusion, we have observed for the first time the Cabibbo-suppressed decays $\Xi_c^0 \rightarrow \Xi^- K^+$, $\Xi_c^0 \rightarrow \Lambda K^+ K^-$ and $\Xi_c^0 \rightarrow \Lambda\phi$ with significances of 8.0σ , 6.4σ and 5.6σ , respectively. The ratios of the branching fractions $\frac{\mathcal{B}(\Xi_c^0 \rightarrow \Xi^- K^+)}{\mathcal{B}(\Xi_c^0 \rightarrow \Xi^- \pi^+)}$, $\frac{\mathcal{B}(\Xi_c^0 \rightarrow \Lambda K^+ K^-)}{\mathcal{B}(\Xi_c^0 \rightarrow \Xi^- \pi^+)}$ and $\frac{\mathcal{B}(\Xi_c^0 \rightarrow \Lambda\phi)}{\mathcal{B}(\Xi_c^0 \rightarrow \Xi^- \pi^+)}$ are measured to be $(2.75 \pm 0.51 \pm 0.25) \times 10^{-2}$, $(2.86 \pm 0.61 \pm 0.37) \times 10^{-2}$ and $(3.43 \pm 0.58 \pm 0.32) \times 10^{-2}$, respectively.

The observed decay modes proceed through external and internal W -emission diagrams with an admixture of the W -exchange diagram. Our results can be used to study the corresponding decay dynamics and to investigate quantitatively the interplay between strong and weak interactions in charmed baryon weak decays. We confirm the previous observations [2, 3, 12] that the W -internal diagrams are not (color) suppressed as compared to the W -external diagrams in charm baryon decays.

We thank the KEKB group for the excellent operation of the accelerator; the KEK cryogenics group for the efficient operation of the solenoid; and the KEK computer group, the National Institute of Informatics, and the PNNL/EMSL computing group for valuable computing and SINET4 network support. We acknowledge support from the Ministry of Education, Culture, Sports, Science, and Technology (MEXT) of Japan, the Japan Society for the Promotion of Science (JSPS), and the Tau-Lepton Physics Research Center of Nagoya University; the Australian Research Council and the Australian Department of Industry, Innovation, Science and Research; the National Natural Science Foundation of China under Contracts No. 10575109, No. 10775142, No. 10875115 and No. 10825524; the Ministry of Education, Youth and Sports of the Czech Republic under Contracts No. LA10033 and MSM0021620859; the Department of Science and Technology of India; the Istituto Nazionale di Fisica Nucleare of Italy; the BK21 and WCU program of the Ministry Education Science and Technology, National Research Foundation of Korea, and GSDC of the Korea Institute of Science and Technology Information; the Polish Ministry of Science

and Higher Education; the Ministry of Education and Science of the Russian Federation and the Russian Federal Agency for Atomic Energy; the Slovenian Research Agency; the Swiss National Science Foundation; the National Science Council and the Ministry of Education of Taiwan; and the U.S. Department of Energy and the National Science Foundation. This work is supported by a Grant-in-Aid from MEXT for Science Research in a Priority Area (“New Development of Flavor Physics”), and from JSPS for Creative Scientific Research (“Evolution of Tau-lepton Physics”).

-
- [1] J. Korner and M. Kramer, *Z. Phys. C* **55**, 659 (1992); K. K. Sharma and R. C. Verma, *Phys. Rev. D* **55**, 7067 (1997).
- [2] K. Abe *et al.* (Belle Collaboration), *Phys. Lett. B* **524**, 33 (2002).
- [3] B. Aubert *et al.* (BABAR Collaboration), *Phys. Rev. D* **75**, 052002 (2007).
- [4] J. Beringer *et al.* (Particle Data Group), *Phys. Rev. D* **86**, 010001 (2012).
- [5] S. Kurokawa and E. Kikutani, *Nucl. Instrum. Methods Phys. Res., Sect. A*, **499**, 1 (2003), and other papers included in this volume; T. Abe *et al.*, *Prog. Theor. Exp. Phys.* 03A001 (2013), and following articles up to 03A011.
- [6] A. Abashian *et al.* (Belle Collaboration), *Nucl. Instrum. Methods Phys. Res. Sect. A* **479**, 117 (2002); also see detector section in J. Brodzicka *et al.*, *Prog. Theor. Exp. Phys.* 04D001 (2012).
- [7] D. Lange, *Nucl. Instrum. Methods. Phys. Res., Sect. A* **462**, 152 (2001); T. Sjöstrand *et al.*, *Comput. Phys. Commun.* **135**, 238 (2001).
- [8] R. Brun *et al.*, GEANT 3.21, CERN Report No. DD/EE/84-1, 1984.
- [9] R. Chistov *et al.* (Belle Collaboration), *Phys. Rev. D* **74**, 111105 (2006).
- [10] T. Lesiak *et al.* (Belle Collaboration), *Phys. Lett. B* **605**, 237 (2005); *Phys. Lett. B* **617**, 198(E) (2005).
- [11] E. Solovieva *et al.* (Belle Collaboration), *Phys. Lett. B* **672**, 1 (2009).
- [12] B. Aubert *et al.* (BABAR Collaboration), *Phys. Rev. Lett.* **95**, 142003 (2005).

TABLE I: Summary of systematic errors in the ratios of $\frac{\mathcal{B}(\Xi_c^0 \rightarrow \Xi^- K^+)}{\mathcal{B}(\Xi_c^0 \rightarrow \Xi^- \pi^+)}$ ($\Xi^- K^+$), $\frac{\mathcal{B}(\Xi_c^0 \rightarrow \Lambda K^+ K^-)}{\mathcal{B}(\Xi_c^0 \rightarrow \Xi^- \pi^+)}$ ($\Lambda K^+ K^-$) and $\frac{\mathcal{B}(\Xi_c^0 \rightarrow \Lambda \phi)}{\mathcal{B}(\Xi_c^0 \rightarrow \Xi^- \pi^+)}$ ($\Lambda \phi$).

Source	Value, % ($\Xi^- K^+$)	Value, % ($\Lambda \phi$)	Value, % ($\Lambda K^+ K^-$)
Kaon ID	1	2	2
Fit model	9	8	7
Interference	...	3.8	3.8
MC statistics	0.5	0.5	0.5
MC model	2
MC width	10
Total	9.1	9.1	13.1